

# Laser Absorption Measurements of H<sup>35</sup>Cl in a Shock Tube for Investigating the Chemical Kinetics of Rocket Propellants

Claire M. Grégoire, Eric L. Petersen

J. Mike Walker '66 Department of Mechanical Engineering, Texas A&M University  
College Station, Texas, USA

## 1 Introduction

Rockets are extensively utilized to deliver satellites that ensure the function of many applications such as cell phones, TV programs, weather forecasts, and GPS, to cite a few, along with the possibility of exploring the solar system. Ammonium Perchlorate (AP)-based composite propellants are extensively used in propulsion applications, spanning from the field of aerospace to military-critical technical weapons [1]. The decomposition of ammonium perchlorate is initiated by  $\text{NH}_4\text{ClO}_4 \rightarrow \text{NH}_3 + \text{HClO}_4$ , leading to the formation of two main compounds: ammonia ( $\text{NH}_3$ ) and perchloric acid ( $\text{HClO}_4$ ) [2,3]. There is a significant lack of studies in the literature detailing how  $\text{HClO}_4$  combustion occurs and even fewer studies on how chlorinated species ( $\text{HCl}$ ) and radical ( $\text{Cl}$ ) interact with  $\text{NH}_3$  and the solid rocket fuel binder into which the AP is typically embedded. To this end, a proposed surrogate that consists of a mixture with  $\text{NH}_3$ ,  $\text{CH}_4$  (a fuel representative for the propellant binder), and trichloromethane ( $\text{CHCl}_3$ ) was tested for the first time. The selection of  $\text{CHCl}_3$  as the precursor species was based on its rapid decomposition, releasing a significant amount of  $\text{HCl}$  and  $\text{Cl}$  that can react with the two other parent molecules  $\text{NH}_3$  and  $\text{CH}_4$ , meanwhile reducing the safety risk relative to attempting the vaporization of  $\text{HClO}_4$  directly in our experimental setup. Therefore, the oxidation of  $\text{NH}_3/\text{CH}_4/\text{CHCl}_3$  at  $\phi = 1.0$  in 99.5% Ar was studied in a shock tube for temperatures ranging from 1475 to 2338 K, and near-atmospheric pressure. The recent development of a  $\text{HCl}$  laser absorption diagnostic enables the measurement of  $\text{HCl}$  time-history profiles behind reflected shock waves [4]. These experimental results provide unique target data to develop and validate a new chemical kinetics reaction mechanism—that are much required for the AP gas-phase combustion processes [5]—assembled for this work. The current model presented in this study contains 3397 reactions and 407 species and was compiled from the following existing models:

- 1) The Halon 1211 ( $\text{CF}_2\text{BrCl}$ ) mechanism from Mathieu *et al.* [6], where the chlorinated hydrocarbon sub-mechanisms and  $\text{CH}_4$ -Cl chemistry are available with a total of 2498 reactions and 319 species;

2) The  $\text{NH}_3\text{-N}_2\text{O}$  mechanism from Mathieu *et al.* [7], which is suitable for understanding the detailed  $\text{NH}_3$  sub-mechanisms and its behavior in blended combinations with hydrocarbons, with 874 reactions and 84 species.

3) The reactions involving N-Cl interactions that were found in three AP chemical kinetics mechanisms, namely the Gross [8], Giovangigli *et al.* [9], and Chen and McQuaid [10] models, which represent 25 reactions and required the addition of new species, such as  $\text{NOCl}$ , see Table 1.

Table 1: Reactions involving N-Cl interactions found in the literature [8-10] that were implemented in the tentative model presented in this study.

Model	Gross [8] 9 Reactions	Giovangigli et al. [9] 9 Reactions	Chen and McQuaid [10] 7 Reactions
Reactions	$\text{ClO} + \text{NO} \rightleftharpoons \text{Cl} + \text{NO}_2$ $\text{ClO} + \text{NH}_3 \rightleftharpoons \text{HOCl} + \text{NH}_2$ $\text{NH}_3 + \text{Cl} \rightleftharpoons \text{NH}_2 + \text{HCl}$ $\text{NH}_2 + \text{ClO} \rightleftharpoons \text{HNO} + \text{HCl}$ $\text{ClO}_2 + \text{NO} \rightleftharpoons \text{ClO} + \text{NO}_2$ $\text{Cl} + \text{N}_2\text{O} \rightleftharpoons \text{ClO} + \text{N}_2$ $\text{ClO} + \text{HNO} \rightleftharpoons \text{HCl} + \text{NO}_2$ $\text{Cl} + \text{NH}_2 \rightleftharpoons \text{HCl} + \text{NH}$ $\text{ClO}_2 + \text{NH} \rightleftharpoons \text{ClO} + \text{HNO}$	$\text{NOCl} + \text{M} \rightleftharpoons \text{NO} + \text{Cl} + \text{M}$ $\text{NOCl} + \text{H} \rightleftharpoons \text{NO} + \text{HCl}$ $\text{NOCl} + \text{O} \rightleftharpoons \text{ClO} + \text{NO}$ $\text{ClOH} + \text{NH} \rightleftharpoons \text{NOCl} + \text{H}_2$ $\text{Cl}_2 + \text{NO} \rightleftharpoons \text{NOCl} + \text{Cl}$ $\text{NOCl} + \text{ClO} \rightleftharpoons \text{NO}_2 + \text{Cl}_2$ $\text{Cl} + \text{NH} \rightleftharpoons \text{HCl} + \text{N}$ $\text{NH}_3 + \text{ClOH} \rightleftharpoons \text{NH}_2\text{OH} + \text{HCl}$ $\text{NH}_2\text{OH} + \text{ClO} \rightleftharpoons \text{ClOH} + \text{HNOH}$	$\text{ClO} + \text{NH}_2 \rightleftharpoons \text{Cl} + \text{H}_2\text{NO}$ $\text{ClO} + \text{H}_2\text{NO} \rightleftharpoons \text{ClOH} + \text{HNO}$ $\text{ClO} + \text{NO} + \text{M} \rightleftharpoons \text{Cl} + \text{NO}_2 + \text{M}$ $\text{NOCl} + \text{H}_2\text{O} \rightleftharpoons \text{HONO} + \text{HCl}$ $\text{NOCl} + \text{NO} \rightleftharpoons \text{ClO}_2 + \text{N}_2$ $\text{ClOH} + \text{HNO} \rightleftharpoons \text{HCl} + \text{HONO}$ $\text{ClO}_2 + \text{HNO} \rightleftharpoons \text{HOCIO} + \text{NO}$

This paper is organized as follows: the experimental methods, i.e. the shock-tube facility and the laser absorption diagnostic, are introduced first. Then, the new oxidation results of the AP surrogate are presented and compared with the current model. The mechanism performance is discussed, and, finally, routes for improvements on predicting this major intermediate species, i.e.  $\text{HCl}$ , are suggested. By strengthening the fundamental database available for the combustion kinetics of AP-based composites, the investigation of the solid rocket propellants can be more efficient, while bringing to light its current limitations, soon to be explored further.

## 2 Experimental Method

### a Shock-Tube Facility

The Low-Pressure Shock Tube (LPST) at Texas A&M University is a stainless-steel facility designed for chemical kinetics measurements and implemented to produce low-pressure conditions allowing for laser absorption experiments. The driver section has a 7.62-cm inner diameter and is 2-m long, while the driven section has a 10.8-cm square inner dimensions and is 4-m long. These two parts are separated by a single, polycarbonate diaphragm, and a cross-shaped cutting blade is used to facilitate the diaphragm's rupture and initiate shock propagation. In fact, the "driver gas", usually He (due to its high efficiency), relaxes towards the low-pressure section, creating a succession of compression waves, eventually forming a shock wave. Thanks to this wave, it is possible to raise abruptly the temperature and the pressure of the gas to be studied for a few milliseconds. The final temperature  $T_5$  and pressure  $P_5$  behind the reflected shock wave were calculated using a code based on the 1-D normal shock equations within uncertainties of  $\pm 1\%$  and  $\pm 0.8\%$ , respectively. Detailed calculations on temperature uncertainty in shock tubes are well-documented in Petersen *et al.* [11]. To measure the incident-shock velocity, four piezoelectric pressure transducers (PCB P113B22) were employed to detect non-intrusively the shock passage

over the last 2 m of the shock tube, producing three incident-shocks velocity measurements. With a well-known spacing between the four PCBs, this configuration allows a linear fit through the measured velocities to be extrapolated and to estimate the incident-shock velocity once it reaches the endwall. To maintain high purity for chemical kinetics experiments, the shock tube has a vacuum system utilizing a rotary vane pump (Agilent DS 402) and a turbomolecular pump (Agilent Turbo V1001 Navigator) to achieve pressures of  $10^{-5}$  Torr or less prior to each test. Lastly, the oxidation of the AP surrogate is executed with liquid  $\text{CHCl}_3$  from Sigma Aldrich with a purity  $\geq 99.8\%$ , and all the gases from Linde with high purities:  $\text{CH}_4$  (99.97%),  $\text{NH}_3$  (99.995%), and  $\text{O}_2$ -He-Ar (99.999%). Table 2 summarizes the experimental conditions for the surrogate mixture  $\text{CHCl}_3/\text{CH}_4/\text{NH}_3$ ,  $\phi = 1.0$  in 99.5% Ar. The oxidation mixture was computed with the combustion reaction defined as follows:  $\text{CHCl}_3 + \text{NH}_3 + \text{CH}_4 + 3.25 \text{O}_2 \rightarrow 2 \text{CO}_2 + 2.5 \text{H}_2\text{O} + 3 \text{HCl} + 0.5 \text{N}_2$ , with HCl as a final product, according to equilibrium calculations. Lastly, the abundance of the isotope  $\text{H}^{35}\text{Cl}$  was detected with similar proportions mentioned in Grégoire and Petersen [12], namely  $[\text{H}^{35}\text{Cl}] \approx 3 \times [\text{H}^{37}\text{Cl}]$ .

Table 2: Mixture composition for  $\text{CHCl}_3/\text{CH}_4/\text{NH}_3$  at  $\phi = 1.0$  in 99.5% Ar with  $T_5$  and  $P_5$  details.

$X_{\text{CHCl}_3}$	$X_{\text{CH}_4}$	$X_{\text{NH}_3}$	$X_{\text{O}_2}$	$X_{\text{Ar}}$	$T_5$ (K)	$P_5$ (atm)
0.0008	0.0008	0.0008	0.0026	0.995	1475-2338	1.10-1.52

#### b $\text{H}^{35}\text{Cl}$ Laser Absorption Diagnostic

The measurements of  $\text{H}^{35}\text{Cl}$  time-history profiles are performed using a distributed-feedback (DFB) interband cascade laser (ICL) from Nanoplus GmbH, producing light near  $3.3 \mu\text{m}$  and tuned at  $3045.06 \text{ cm}^{-1}$ , corresponding to the R(8) transition line of  $\text{H}^{35}\text{Cl}$  in the fundamental band. The laser beam is initially split into two beams using a 90/10 beam splitter, where 10% of the beam is directed to a wavemeter for wavelength verification (671B-MIR from Bristol Instruments) with an accuracy of  $\pm 0.001 \text{ cm}^{-1}$ . Then, 90% of the beam goes to another 50/50 beam splitter: the first incident intensity ( $I_0$ ) passes a flat mirror, a polarizer, a converging lens, and a bandpass filter to finally get collected to the detector (from Vigo Photonics, model PVI-4TE-8). Similarly, the second transmitted intensity ( $I_t$ ) is collected by another detector passing the same optics and additional mirrors, but also travels through the shock-tube windows. In this context, polarizers are selected to reduce or modify the intensity of the wavelength light in replacement of neutral density filters for their flexibility. Their ease to balance the incident and the transmitted beams when seated on rotation mounts can control the divided intensities precisely. The time-resolved  $\text{H}^{35}\text{Cl}$  mole fractions are retrieved with these two intensities using the Beer-Lambert relation, defined as:

$$\ln(I_t/I_0) = -k_\nu P_5 L X_{\text{H}^{35}\text{Cl}} \quad (1)$$

where  $k_\nu$  is the absorption coefficient,  $P_5$  is the pressure,  $L$  is the path length (shock-tube diameter), and  $X_{\text{H}^{35}\text{Cl}}$  is the mole fraction of  $\text{H}^{35}\text{Cl}$ . The absorption coefficient (in  $\text{cm}^{-1} \cdot \text{atm}^{-1}$ ) in the Beer-Lambert law can be written with two spectroscopic parameters: the line strength ( $S_{12}(T)$ ) and the line shape ( $\phi_\nu$ ), where both parameters are examined in detail in Grégoire and Petersen [12]. Note that the oxidation of the AP surrogate induces an increase in temperature ( $\Delta T_5 = 100\text{-}150 \text{ K}$ ), which is accounted for with an adapted time-varying absorption coefficient.

### 3 Results and Discussion

#### a $\text{CHCl}_3/\text{CH}_4/\text{NH}_3$ Oxidation

The oxidation of  $\text{CHCl}_3/\text{CH}_4/\text{NH}_3$  at  $\phi = 1.0$  highly diluted in 99.5% Ar was carried out for temperatures between 1475 and 2338 K with pressures from 1.29 to 1.55 atm. A representative  $\text{H}^{35}\text{Cl}$  time history is illustrated in Fig. 1 at 2221 K, 1.16 atm, and the two spikes appearing in the  $\text{H}^{35}\text{Cl}$  profile correspond to a temporary beam steering caused by the density change from the passage of the incident and the reflected shock waves. The general features of the  $\text{H}^{35}\text{Cl}$  profile show an immediate release of HCl produced via the reaction  $\text{CHCl}_3 \rightleftharpoons \text{CCl}_2 + \text{HCl}$  (R1), which blends with the second schlieren spike from the reflected shock wave. Sensitivity analyses depict an important production of Cl directly after the decomposition of  $\text{CHCl}_3$  from the reaction  $2\text{CCl}_2 \rightleftharpoons \text{C}_2\text{Cl}_3 + \text{Cl}$  (R2). For these reasons, the authors believe that the surrogate mixture of AP is successfully designed to highlight interactions of  $\text{CH}_4$  and  $\text{NH}_3$  with Cl active radicals. Consequently,  $\text{H}^{35}\text{Cl}$  concentration continues to increase via the reactions  $\text{CH}_4 + \text{Cl} \rightleftharpoons \text{CH}_3 + \text{HCl}$  (R3) and  $\text{NH}_3 + \text{Cl} \rightleftharpoons \text{NH}_2 + \text{HCl}$  (R4) up to 100  $\mu\text{s}$ . Then,  $\text{H}^{35}\text{Cl}$  is eliminated with different reaction sub-mechanisms, notably via the reaction  $\text{HCl} + \text{O} \rightleftharpoons \text{OH} + \text{Cl}$  (R5), further discussed in the next section using the detailed kinetics mechanism presented in this study.

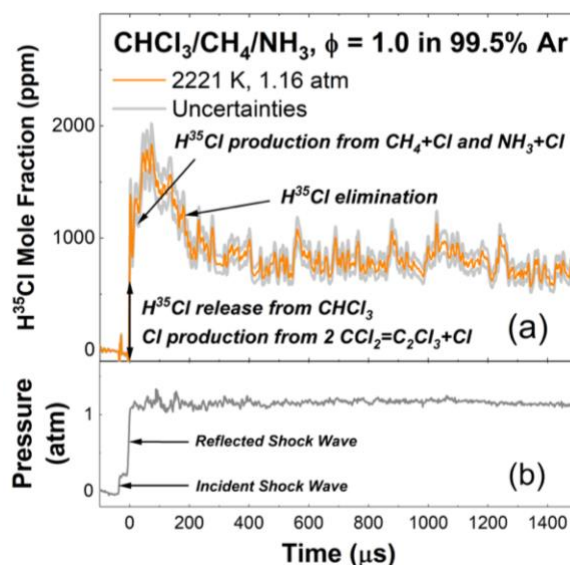


Figure 1: a)  $\text{H}^{35}\text{Cl}$  time-history profile recorded behind reflected shock wave for the oxidation of  $\text{CHCl}_3/\text{CH}_4/\text{NH}_3$  at  $\phi = 1.0$  in 99.5% Ar at 2221 K, 1.16 atm and b) its pressure signal.

#### b. Detailed Kinetics Modeling

Experimental  $\text{H}^{35}\text{Cl}$  profiles (solid lines) are shown in Fig. 2 for high (2045-2338 K), intermediate (1715-1882 K), and low (1475-1565 K) temperatures. Numerical predictions (dashed lines) are compared with the new results, and one can see that the mechanism reproduces the  $\text{H}^{35}\text{Cl}$  profiles with some difficulty. While the detailed mechanism captures the early release of  $\text{H}^{35}\text{Cl}$  from  $\text{CHCl}_3$ , the formation of  $\text{H}^{35}\text{Cl}$  from (R3) and (R4) is not well-understood, as the mechanism is under-reactive for the entire set of experiments, with predicted  $\text{H}^{35}\text{Cl}$  mole fractions roughly 10%

below the experimental results. Note that large discrepancies are observed when the model is evaluated at intermediate temperatures in our conditions due to competitive reactions creating a ‘plateau’, see Fig. 2 (c) where the model slowly increases  $\text{H}^{35}\text{Cl}$  ppm levels from 100  $\mu\text{s}$  up to 700  $\mu\text{s}$  before displaying its decrease. Similar observations can be made using Fig. 2 (d), where the experimental profile demonstrates a fairly constant  $\text{H}^{35}\text{Cl}$  concentration between 200 and 500  $\mu\text{s}$ .

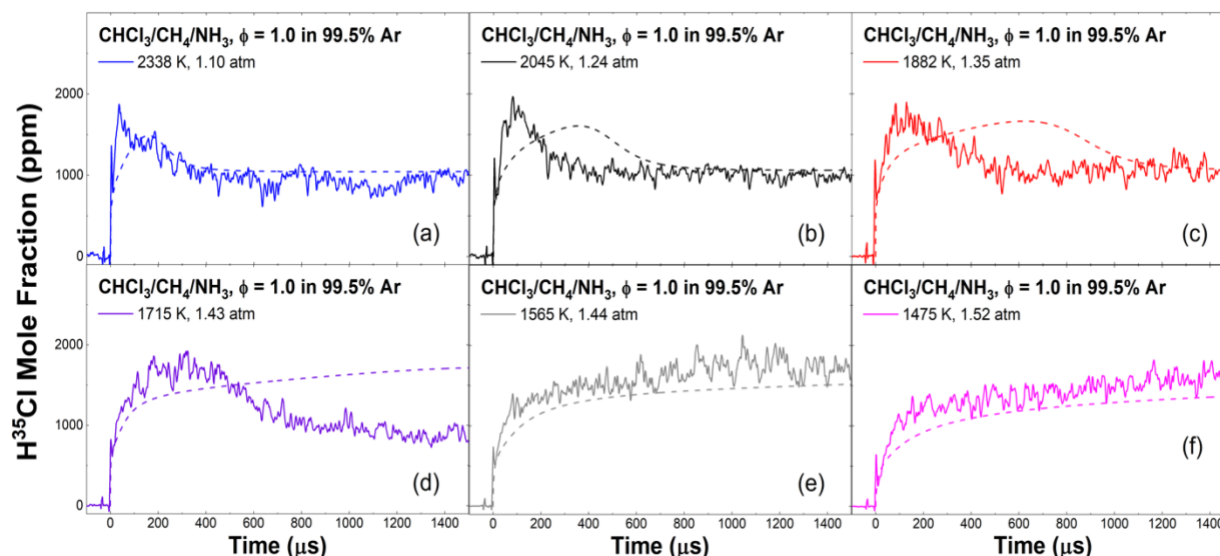


Figure 2:  $\text{H}^{35}\text{Cl}$  time-history profiles recorded behind reflected shock waves for the oxidation of  $\text{CHCl}_3/\text{CH}_4/\text{NH}_3$  at  $\phi = 1.0$  in 99.5% Ar at a) 2338 K, 1.10 atm, b) 2045 K, 1.24 atm, c) 1882 K, 1.35 atm, d) 1715 K, 1.43 atm, e) 1565 K, 1.44 atm, and f) 1475 K, 1.52 atm. Solid and dashed lines represent the experimental measurements and the numerical predictions, respectively.

Sensitivity analyses highlight the importance of the reactions (R1) and (R2) at the very beginning of the test, at the present experimental conditions; later, the reactions (R3) and (R4) play a key role to the additional increase of  $\text{H}^{35}\text{Cl}$ . The detailed mechanism allows the identification of the reaction pathways responsible for the  $\text{H}^{35}\text{Cl}$  ‘plateau’ observed experimentally and numerically in Fig. 2 (d) at 1715 K and in Figs. 2 (b-c) at 1882-2045 K, respectively. The production of  $\text{H}^{35}\text{Cl}$  slows down due to competitive reactions initiated by a secondary pathway for the dichlorocarbene ( $\text{CCl}_2$ ), specifically, the less-sensitive reactions  $\text{CCl}_2 + \text{H} \rightleftharpoons \text{CHCl} + \text{Cl}$  (R6) and  $\text{CCl}_2 + \text{H} \rightleftharpoons \text{CHCl}_2$  (R7). Moreover, the Cl radicals are now reacting with  $\text{CH}_2\text{O}$  and  $\text{NH}$ , i.e.  $\text{CH}_2\text{O} + \text{Cl} \rightleftharpoons \text{HCl} + \text{HCO}$  (R8) and  $\text{NH} + \text{Cl} \rightleftharpoons \text{HCl} + \text{N}$  (R9), supplied by  $\text{CH}_4$  and  $\text{NH}_3$  sub-mechanisms, respectively. Finally, the decrease of  $\text{H}^{35}\text{Cl}$  is driven by (R5), and to a lesser extent, the following reactions:  $\text{HCl} + \text{OH} \rightleftharpoons \text{Cl} + \text{H}_2\text{O}$  (R10) and  $\text{HCl} + \text{H} \rightleftharpoons \text{H}_2 + \text{Cl}$  (R11).

## 4 Conclusion

This paper presents new  $\text{H}^{35}\text{Cl}$  time-history profiles obtained behind reflected shock waves for the study of an AP surrogate mixture that consists of  $\text{CHCl}_3/\text{CH}_4/\text{NH}_3/\text{O}_2$  in 99.5% Ar. The ICL absorption diagnostic was centered at  $3045.06 \text{ cm}^{-1}$  to access the R(8) transition line of  $\text{H}^{35}\text{Cl}$  in the fundamental band, and this technique combined with a shock tube permitted the measurement of  $\text{H}^{35}\text{Cl}$  at temperatures ranging from 1475 to 2338 K at near-atmospheric pressure.  $\text{CHCl}_3$  decomposition releases a significant level of  $\text{H}^{35}\text{Cl}$  from the reaction  $\text{CHCl}_3 \rightleftharpoons \text{CCl}_2 + \text{HCl}$  (R1),

and the  $\text{CCl}_2$  sub-mechanism provides Cl-active radicals via the reaction  $2\text{CCl}_2 \rightleftharpoons \text{C}_2\text{Cl}_3 + \text{Cl}$  (R2). Consequently, Cl interactions are directly observed with  $\text{CH}_4$  and  $\text{NH}_3$ , and sensitivity analyses indicate that the following reactions are taking place:  $\text{CH}_4 + \text{Cl} \rightleftharpoons \text{CH}_3 + \text{HCl}$  (R3) and  $\text{NH}_3 + \text{Cl} \rightleftharpoons \text{NH}_2 + \text{HCl}$  (R4), increasing  $\text{H}^{35}\text{Cl}$  mole fractions even more. Numerical predictions obtained with the tentative, detailed kinetics mechanism proposed in this work exhibit significant discrepancies when compared against the new experimental results. However, further analyses suggest routes of improvement by identifying key reactions, and fine reaction rate tuning could address these poor predictions. The work presented in this paper provides some of the first detailed chemical kinetics data obtained in a shock tube that probes the high-temperature chemistry of the same fundamental ammonia/chlorine/hydrocarbon system as AP/HTPB. To this end, the technique proved successful in highlighting the interactions between the Cl,  $\text{NH}_3$ , and hydrocarbon sub-systems, and it shows much promise for future detailed kinetics studies using AP surrogate precursors.

## References

- [1] Dennis C, Bojko B (2019). On the combustion of heterogeneous AP/HTPB composite propellants: A review. *Fuel* 254: 115646.
- [2] Jeppson M, Beckstead M, Jing Q, A kinetic model for the premixed combustion of a fine AP/HTPB composite propellant, *AIAA J.*, *AIAA Journal*, (1998).
- [3] Beckstead MW, Puduppakkam K, Thakre P, Yang V (2007). Modeling of combustion and ignition of solid-propellant ingredients. *Prog. Energy Combust. Sci.* 33: 497.
- [4] Grégoire C, Laser Absorption Measurements of HCl in a Shock Tube for the Chemical Kinetics Study of Rocket Propellants, Ph.D., Mechanical Engineering, Texas A&M University, (2024).
- [5] Grégoire CM, Mathieu O, Kalman J, Petersen EL (2025). Review and assessment of the ammonium perchlorate chemistry in AP/HTPB composite propellant gas-phase chemical kinetics mechanisms. *Prog. Energy Combust. Sci.* 106: 101195.
- [6] Mathieu O, Keesee C, Gregoire C, Petersen EL (2015). Experimental and Chemical Kinetics Study of the Effects of Halon 1211 ( $\text{CF}_2\text{BrCl}$ ) on the Laminar Flame Speed and Ignition of Light Hydrocarbons. *J. Phys. Chem. A* 119: 7611.
- [7] Mathieu O, Grégoire CM, Petersen EL (2024). Shock-tube study of the oxidation of ammonia by  $\text{N}_2\text{O}$ . *Proc. Combust. Inst.* 40: 105250.
- [8] Gross ML, Two-Dimensional Modeling of AP/HTPB Utilizing a Vorticity Formulation and One-Dimensional Modeling of AP and ADN, Ph.D. Dissertation, Department of Chemical Engineering, Brigham Young University, (2007).
- [9] Giovangigli V, Meynet N, Smooke M (2006). Application of continuation techniques to ammonium perchlorate plane flames. *Combust. Theory Model.* 10: 771.
- [10] Chen C, McQuaid M, A Skeletal, Gas-Phase, Finite-Rate, Chemical Kinetics Mechanism for Modeling the Deflagration of Ammonium Perchlorate-Hydroxyl-Terminated Polybutadiene Composite Propellants, US Army Research Laboratory, US Army Research Laboratory, (2016).
- [11] Petersen EL, Rickard MJA, Crofton MW, Abbey ED, Traum MJ, Kalitan DM (2005). A facility for gas- and condensed-phase measurements behind shock waves. *Meas. Sci. Technol.* 16: 1716.
- [12] Grégoire C, Petersen EL, Development of a HCl Laser Absorption Diagnostic near  $3.3 \mu\text{m}$  for Shock-Tube Chemical Kinetics Studies, *Applied Physics B*, (Submitted), pp. Submitted.